Generated using the official AMS LaTeX template v6.1

This is a non-peer reviewed preprint that has been submitted to *Journal of Atmospheric Sciences*; future versions may have different content.

The relation between European heat waves and North Atlantic SSTs: a two-sided composite analysis

Julian Krüger,[a] Joakim Kjellsson,[a,b] Robin Pilch Kedzierski,[a] Martin Claus[a,b]

[a] *GEOMAR Helmholtz Centre for Ocean Research, Kiel, Germany*

[b] *Christian-Albrechts-University, Kiel, Germany*

Corresponding author: Julian Krüger, jukrueger@geomar.de

ABSTRACT: The occurrence of European heat waves has increased during the two last decades. European heat waves are responsible for social, economic and environmental damage and are projected to increase in magnitude, frequency and duration under global warming, heightening the interest about the contribution of different drivers.

By using the ERA5 Re-analysis product, we performed a two-sided composite analysis to investigate a potential relation between North Atlantic sea surface temperatures (SSTs) and the near-surface air temperature (T2m) over the European continent. Here, we show that in presence of cold North Atlantic SSTs during summer, the distribution of European T2m shifts towards positive anomalies a few days later, increasing the likelihood for heat waves (Downstream analysis). During these events a predominant wave number three pattern in addition to regionally confined Rossby wave activity contribute to a trough-ridge pattern in the North Atlantic-European sector. Specifically, five of 17 European heat waves within the period of 1979 to 2019 could be related to a cold North Atlantic SST event a few days in advance. In the upstream analysis we identify eleven of 17 European heat waves co-existent with below-average North Atlantic SSTs, including five cold North Atlantic SST events.

Based upon our results North Atlantic SSTs provide potential predictive skill of European heat waves.

SIGNIFICANCE STATEMENT: This study aims to find a relationship between North Atlantic sea surface temperatures and Central European heat waves. The elaboration of European heat waves and its drivers are important, as European heat waves have a wide range of impacts and their occurrence has increased in the two recent decades.

Our results highlight that cold North Atlantic sea surface temperatures are associated with a surface air temperature maximum over Central Europe a few days later, increasing the probability for heat waves. In future, the role of North Atlantic sea surface temperatures as a potential driver needs to be further investigated, as they would provide an increased predictability range of European heat waves.

1. Introduction

The European continent experienced an increased number of notable heat waves during the two recent decades (Christidis et al. 2015; Coumou et al. 2013). Past heat waves had severe impacts on the environment, e.g., fire hazards and water shortages as well as on society, e.g., agricultural losses, heat stress on human health and excess mortality (Sun et al. 2019; Miller et al. 2021).

The origins and effects of several European heat waves have been thoroughly studied by the scientific community. In summer 1994 Central and Eastern Europe experienced excessively hot conditions as illustrated by Lhotka and Kyselý (2015) and Röthlisberger et al. (2019). Numerous authors reported on the well-known European heat wave in 2003 (García-Herrera et al. 2010; Stott et al. 2004; Black et al. 2004; Fischer et al. 2007), which led to an excess mortality of 70,000 deaths (Robine et al. 2008). Eastern Europe and large parts of Russia were exceptionally warm during the summer of 2010, recording additional 55,000 deaths related to this heat event (Barriopedro et al. 2011; Grumm 2011). Another heat period evolved in Western Europe in late June 2015 and spread towards Southern and Eastern Central Europe (Duchez et al. 2016; Mecking et al. 2019; Dong et al. 2016). Prolonged heat wave conditions affected large parts of Europe with the centre over Scandinavia in the 2018 summer season (Kueh and Lin 2020; Sinclair et al. 2019; McCarthy et al. 2019; Dunstone et al. 2019).

Several studies provide strong evidence for an observed increase in the occurrence of heat waves due to the anthropogenically induced climate change (Coumou and Rahmstorf 2012; Stott et al. 2016; Diffenbaugh et al. 2017; Mann et al. 2018). A strengthened temperature variability (no change of the mean) of the European summer climate (Schär et al. 2004) as well as a general shift of the distribution (change of the mean) towards higher values (Donat and Alexander 2012) both lead to an increase in the probability for and the intensity of a heat wave occurrence (Thornton et al. 2014).

With the aim of improving predictability, it's essential to disentangle the contributions of different mechanisms leading to a heat wave. In general, heat wave drivers need to at least partially contribute to the establishment of persistent above-average temperatures accompanied by the prevalence of an atmospheric ridge (anticyclone) with clear-sky conditions facilitating a net surface heating lasting for several days.

Heat waves can generally evolve through dynamical and thermodynamical drivers (Suarez-Gutierrez et al. 2020). In the context of dynamical drivers, Cassou et al. (2005) highlight that two specific summertime atmospheric circulation regimes significantly favour extreme warm days over Europe. One regime is associated with the Blocking pattern over the continent, which is mainly characterised by a persistent split of the jet flow involving a sharp transition from the prevailing zonal to a dominating meridional flow (Liu 1994). The other regime is the Atlantic Low pattern featured by an anomalously deep trough over the North Atlantic Ocean, while ridge conditions appear over the European continent. This state facilitates the advection of warm air masses from northern Africa and the Mediterranean basin into western and central Europe, increasing the probability for heat events (Cassou et al. 2005).

Another potential dynamical driver of European heat waves could be associated with atmospheric Rossby waves, which tend to propagate zonally in organized so-called Rossby wave packets (RWP) (Chang 1993; Lee and Held 1993). A RWP exists when the amplitude of a Rossby wave varies with longitude such that it reaches a maximum over a certain longitude with a gradual decay both westward and eastward (Wirth et al. 2018). With the characteristic of a finite number of troughs and ridges and a zonal limitation, RWP are still able to favour or even initiate extreme weather events (Fragkoulidis et al. 2018). Temperature extremes could be assigned to a local waviness in a certain longitudinal band than to a hemispheric-wide wave pattern (Röthlisberger et al. 2016). For instance, a recurrence of transient RWPs was observed during the European heat wave of 1994 (Röthlisberger et al. 2019) and during the Russian heat wave of 2010 (Pilch Kedzierski et al. 2020).

Amongst thermodynamical drivers we need to mention the soil moisture availability. The studies by Black et al. (2004) and Fischer et al. (2007) suggested that a lack of soil moisture and evaporative cooling combined with surface feedbacks including latent and sensible heat fluxes strongly contribute to the development of heat waves. Such an excessive drying of the soil was particularly important for the heat waves of 2003 in Europe (Fischer et al. 2007) and 2010 in Russia (Hauser et al. 2016).

Another thermodynamical driver is related to diabatic heating. Ascending airstreams in North Atlantic cyclones associated with latent heat release provide a source for the onset and strengthening of an upper level ridge over Europe (Steinfeld and Pfahl 2019; Steinfeld et al. 2020). This heating branch reaching from the North Atlantic surface into the upper troposphere over Europe could be connected to European heat waves as well (Zschenderlein et al. 2019, 2020).

Dynamical drivers may be connected to ocean variability (Brönnimann 2007). Duchez et al. (2016) observed that the central European heat wave in 2015 was preceded by negative North Atlantic SST anomalies. A similar state of temperature anomalies was identified prior to the European heat wave in 2018 (Mecking et al. 2019). Both heat waves in 2015 and 2018 were associated with a zonally orientated dipole pattern of surface temperature anomalies and an atmospheric trough-ridge pattern over the North Atlantic-European sector, which begs the question of whether cold North Atlantic SSTs could favour the establishment of high pressure and temperature extremes downstream over central Europe and if low-frequency ocean variability could modulate the frequency of European heat waves.

In our study, we focus on the question whether the conditions found in summer 2015 and 2018 including cold North Atlantic SST anomalies and a subsequent trough-ridge pattern in the North Atlantic-European sector were recurrent characteristics of different European heat waves. Here, we seek to find common features of multiple heat wave occurrences, which differs from previous case-studies focussing on individual events (Duchez et al. 2016; Röthlisberger et al. 2019; Mecking et al. 2019; McCarthy et al. 2019). Therefore, we performed a two-sided (up- and downstream) composite analysis obtaining an estimate about the spatio-temporal relationship between North Atlantic SSTs and the European surface temperatures during boreal summer. By using the ERA5-Re-analysis product, we study the contribution of both thermodynamical drivers, e.g. heat fluxes, and dynamical drivers, e.g. propagating planetary waves and RWPs.

2. Methodology

a. ERA5 Re-analysis

We use data from the ERA5 Re-analysis product provided by the European Centre for Medium-Range Weather Forecasts (ECMWF) (Hersbach et al. 2020). Our analysis is based on two-dimensional fields of the geopotential height at 300hPa (Z300), the sea surface temperature (SST), the 2m-air temperature (T2m), surface latent and sensible heat fluxes, surface net solar and thermal radiation, evaporation, large-scale precipitation as well as low, medium, high and total cloud cover. The data was retrieved on a 2.5° longitude x 2.5° latitude horizontal resolution.

We restrict the composite analysis to daily average values of June, July and August (JJA) in the period from 1979 to 2019. All data is detrended to ensure that no potential underlying trend would lead to a bias in the results, compositing more extreme heat episodes occurring later in the studied period. We also remove the daily climatology from the data.

b. Composites

We perform a two-sided composite analysis to investigate the relationship between North Atlantic SST events and European heat waves. The first downstream analysis is based on North Atlantic SST events and an investigation of a potential downstream response over Europe. The second upstream analysis involves the selection of warm European T2m events and the study of the associated North

Atlantic SST anomalies. The details of the downstream and upstream analysis are further described now.

1) Downstream analysis: North Atlantic SST events

For the downstream analysis, we average the SST over a North Atlantic box (15 - 40°W, 45 - 60°N) (Fig. 1) coinciding with the area used by Duchez et al. (2016), where the strongest negative anomalies were found during the European heat wave of 2015.

Based on the distribution of daily JJA values of this North Atlantic SST box average between 1979 and 2019 we classify cold and warm North Atlantic SST events by using the 0.1 and 0.9 quantiles of daily JJA North Atlantic SST anomalies. Additionally, neutral events are defined as SST anomalies within the 0.4 and 0.6 quantiles, delineating the medium SST composite.

We collect only the events which fulfill all following criteria regarding intensity (1), duration (2) and frequency (3), described here based on the example of cold SST events:

1. We identify the first day on which the value falls below the 0.1 quantile (threshold) as the start date.
2. The SST anomaly remains below the threshold for five consecutive days in order to eliminate short-lived anomalies.
3. The start date of two cold SST events are at least 30 days apart in order to avoid overlap between events in the composites.

These criteria are analogously applied to medium and warm SST events. We identify eleven cold events, 13 warm events and 39 medium events based on these criteria from 1979 to 2019 (Fig. 1c, Table 1). We seek to analyse different parameters based on the respective dates of cold, warm and medium composites. These parameters are time-filtered by applying a seven-day running mean.

2) Upstream analysis: European T2m events

For the upstream analysis we select European heat events and evaluate the upstream behaviour before, during and after these events. Due to the higher frequency variability of European T2m compared to the SST data, we apply a seven-day running mean to the T2m data before identifying cold and warm events in an analogous way to the North Atlantic SST events in the downstream analysis. Here we use the European box average (45 - 52.5°N, 0 - 20°E) and apply the same criteria with identical quantile thresholds as for SST events above. We focus solely on the analysis of warm T2m events and neglect the cold and medium T2m events. We identify 17 warm T2m events over Europe (Table 1).

c. Wave filtering

For the wave analysis (section 4), we first perform a fast Fourier transform (FFT) in longitude for the Z300 field. Subsequently, we decompose it into contributions of Planetary waves (PW) defined as zonal wave numbers one to three and synoptic-scale Rossby wave packets defined as intermediate wave numbers (wave numbers four to 15) in agreement with previous studies (Wirth et al. 2018; Zimin et al. 2003; Wolf and Wirth 2017).

d. Significance and robustness test

With respect to the significance of the results, i.e. the assessment of whether a composite based on cold SST events is significantly different from the composite based on medium SST events, we use the Welch's T-test, which is a two-sided test for the null hypothesis that two independent samples have identical average values, assuming that the samples may have different variances. In this study we apply the test to the samples of cold and warm composites with respect to the reference sample, the medium composite, respectively.

Regarding the robustness of the results, we support our analysis with illustrations in terms of probabilities, i.e. the fraction of anomalies that are positive or negative at a given location and time, e.g., the fraction of positive T2m anomalies in a composite of cold SST events. This is separately determined for probabilities of positive and negative anomalies.

3. Statistical relationship between North Atlantic SSTs and European T2m

European heat waves in 2015 and 2018 provide examples of warm T2m anomalies over Europe and associated cold SST anomalies over the North Atlantic ocean (Fig. 1). Particularly, between 12 July to 08 August 2018 the North Atlantic SST anomalies reached negative values of up to -2.5°C, while the T2m was remarkably high over Scandinavia and central Europe with anomalies of up to +4°C compared to the climatology during this period (Fig. 1a).

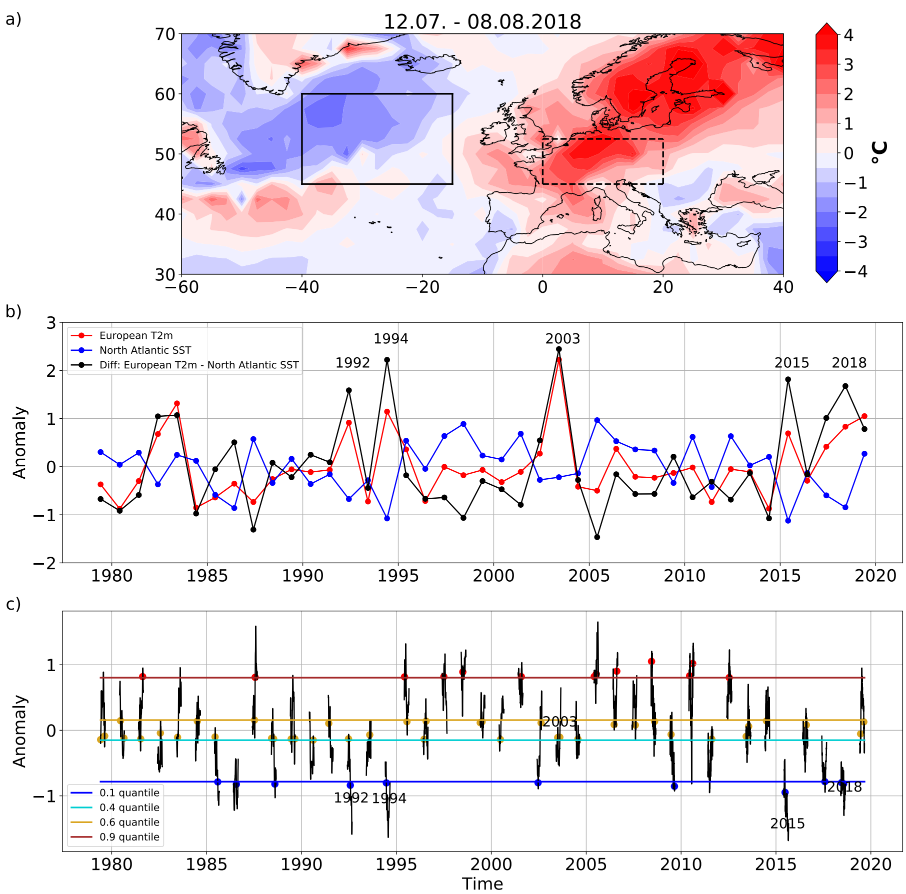

Fig. 1. a) 12.07 - 08.08.2018 anomalies of SST (ocean) and T2m (continent) after removing daily climatology and long term trend from whole time series; North Atlantic box (15 - 40°W, 45 - 60°N) and European box (0 - 20°E, 45 - 52.5°N) used for subsequent average; b) Deseasoned and detrended JJA mean values for North Atlantic (blue) and European box average (red) and difference (black); seasons of outstanding differences are highlighted; c) Deseasoned and detrended daily JJA SST values (black); quantiles (horizontal lines) and composite dates for cold SST events (blue dots), warm SST events (red dots) and medium SST events (orange dots) as well as European heat wave years highlighted.

We study summer seasonal mean (JJA) anomalies by using the same North Atlantic box as Duchez et al. (2016) as well as a European box covering large parts of central Europe (Fig. 1b) and find that the North Atlantic SST and the European T2m exhibit an overall anti-correlation.

Prominent heat wave years (1992, 1994, 2003, 2015, 2018) have a large difference ΔT = T2m - SST between the North Atlantic SST and the European T2m average. We note that the large ΔT in 2003 is mostly caused by a strong positive T2m anomaly and a very small negative North Atlantic SST anomaly.

TABLE 1. List of cold North Atlantic SST (box average: 45 -60°N, 15 - 40°W) events (eleven events) for the downstream analysis and of warm European T2m (box average: 45 - 52.5°N, 0 - 20°E) events (17 events) for the upstream analysis; bold highlighted dates indicate a match between both parameters.

Cold North Atlantic SST events	Warm European T2m events
1985-08-03	1982-07-10
1986-07-27	1983-07-06
1988-08-06	1991-07-05
1992-07-28	**1992-08-03**
1994-06-21	**1994-06-25**
	1996-06-05
2002-06-19	**2002-06-15**
2009-08-26	2003-08-02
	2005-06-18
	2006-06-14
	2006-07-16
	2010-07-09
2015-06-25	**2015-07-01**
2017-07-29	2015-08-06
2018-06-16	2017-06-17
2018-07-26	**2018-07-27**
	2019-06-22

Using the daily JJA values and defining events based upon the quantiles as well as composite criteria mentioned in section 2b, we identify the respective cold and warm SST events (Fig. 1c). A noteworthy aspect of the temporal distribution of the composite dates is that five of eleven cold SST events lie within 1985 to 1995 and only two events are detected within the following 15 years. Instead, for the warm SST composite, there is only one event within 1985 to 1995 and seven events within the subsequent 15-year period. Such a temporally uneven distribution between cold and warm composites indicates an imprint of the Atlantic multi-decadal variability (AMV) (Sutton and Hodson 2005). The uneven distribution of data points between the cold and warm composite supports the necessity of the removal of a long term trend (linear) for parameters based on these composite dates.

The aforementioned years of large ΔT (1992, 1994, 2003, 2015, 2018) all contribute with at least one event to the cold SST composite, except for the heat wave in 2003, which reflects a strong positive seasonal European T2m anomaly, but only a weak negative North Atlantic SST anomaly.

A comparison of the eleven dates of the cold North Atlantic SST composites used for the downstream analysis with the 17 composite dates generated for the upstream analysis evinces five dates, which could be related to each other (Table 1). For the specific cold SST events in 1992, 1994, 2015 and 2018 we obtain a matching European T2m warm event one to six days later. In 2002, there is a date matching as well, but the start date of the cold SST event occurs four days after instead of preceding the European T2m event. Nevertheless these dates might not be unrelated to each other, as the North Atlantic SST could have already been negative, varying around the 0.1 quantile threshold before the start date of the European heat wave is reached.

We draw the conclusion that five out of 17 European heat waves could be temporally related to a cold North Atlantic SST event and that almost half of the cold North Atlantic SST events can be related to a European heat wave. In the following, we attempt to evaluate the spatio-temporal relationship between the North Atlantic SST anomalies and central European T2m anomalies during all events using a lead-lag analysis.

4. Composite analysis

a. Downstream analysis of North Atlantic SST events

In the downstream analysis we study the behaviour of the North Atlantic SST composite events individually as well as in a composite mean. For completeness and for the purpose to check whether a linear response exists, we analyse the composite of cold events as well as of medium and warm events.

We display the temporal behaviour of anomalies of the North Atlantic SST, the European T2m and Z300 over both the North Atlantic and Europe during cold and warm SST events, respectively (Fig. 2). The blue area delineates the time period (SST event onset (0) to five days afterwards), where the warm, cold and medium SST events need to be above, below or within the quantile thresholds, respectively.

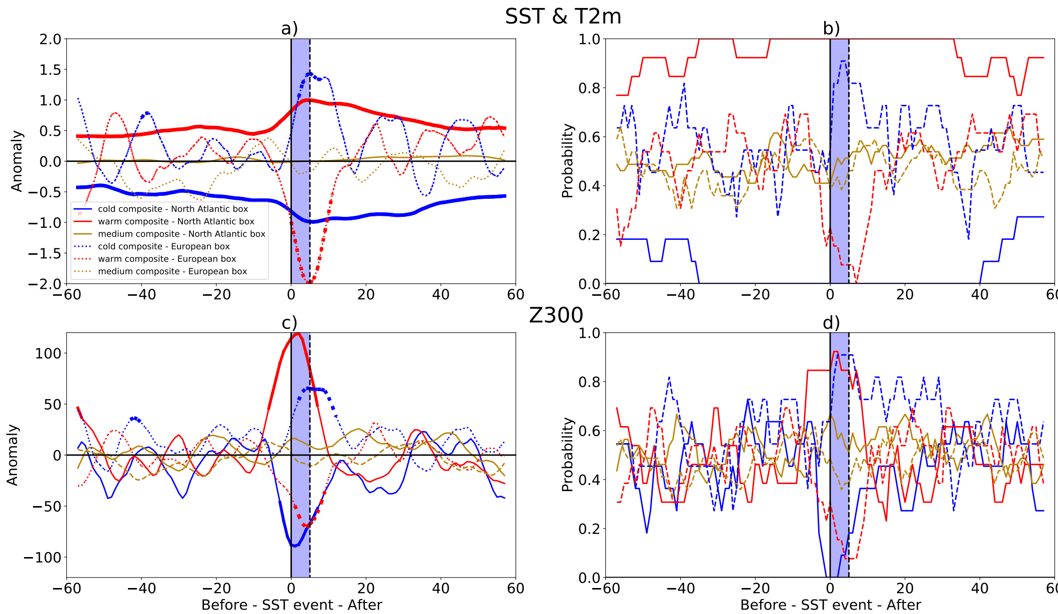

FIG. 2. a) North Atlantic SST (15 - 40°W, 45 - 60°N) (solid lines) and European T2m (0 - 20°E, 45 - 52.5°N) (dashed lines) anomalies during cold (blue), warm (red) and medium (orange) SST events; b) Same as a) but for probabilities of positive SST/T2m anomalies; c) Same as a) but for Z300 anomalies of both North Atlantic and Europe; d) Same as c) but for probabilities of positive Z300 anomalies; the light blue area highlights the range, where SST values have to be at least above (for warm composite), below (for cold composite) or within (for medium composite) the quantile threshold(s) (see section 2b); significant values according to a Welch's test (see section 2d) have a thick line width.

During cold (warm) North Atlantic SST events, the SST anomalies are not only negative (positive) within this range, but also throughout the entire length of the composite (120 days) (Fig. 2a), suggesting that these persistent anomalies emerge either through slow ocean variability or through integration of heat fluxes driven by the atmosphere.

In general, the strongest T2m and Z300 anomalies of the cold and warm North Atlantic SST composite mean are found close to, or within lags 0-5 days (highlighted blue area in Fig. 1). Further, the Z300 is in line with the picture of surface temperature anomalies: the strongest negative North Atlantic SST box average anomalies of -1°C occur at and directly after lag 0 and are co-existent with a trough (-90 gpm) over this region, while some days later the European T2m exhibits significant positive anomalies of almost +1.5°C for roughly one week under the existence of a ridge (+110 gpm) building up over central Europe (Fig. 2a,c). These results are temporally consistent with our previous findings that some European heat waves occur a few days after the start date of a cold North Atlantic SST event (Table 1).

Regarding the warm North Atlantic SST events, we observe the opposite signature, i.e. significant negative T2m anomalies of -2°C are accompanied by a trough (-70 gpm) over central Europe, suggesting an approximately linear response (Fig. 2a,c). The amplitudes of the medium composite are generally weaker and do not pose an outstanding anomaly for any parameter. Note the larger sample size of the medium composite compared to the cold and warm composite.

In order to confirm the robustness of our results, we repeat the analysis in terms of probability. At long lead/lags the probability of warm and cold SST anomalies or high and low Z300 anomalies are ~50%, i.e. equally probable (Fig. 2b,d). We observe a high probability for positive T2m anomalies and high Z300 anomalies over central Europe after a cold SST event. The probabilities indicate atmospheric ridge conditions (Fig. 2d) with positive T2m anomalies (Fig. 2b) persisting for approximately a week in at least 80% of all cold North Atlantic SST cases.

We now illustrate the probabilities of positive Z300 anomalies between 15 - 40°W (Fig. 3a) and 0 - 20°E (Fig. 3b) along with >80% probability of positive and negative SST and T2m anomalies. In the composite of cold SST events the probabilities for positive Z300 anomalies are close to zero over the North Atlantic around lag 0 between 50 to 65°N, suggesting no preference for a ridge at all (Fig. 3a). Contrarily, we observe a rapid increase of probabilities for positive Z300 anomalies after the cold SST event onset over Central Europe (Fig. 3b). The probabilities rise from 0.5 to above 0.8 in the latitude range 40 to 55°N within only a few days. High probabilities for positive European T2m march in step, proposing the generation of above average surface temperature conditions over Europe in at least nine of eleven cold SST events.

In the presence of warm SSTs, we observe higher probabilities for positive Z300 anomalies with values above 0.8 around lag 0 in the North Atlantic (Fig. 3c), indicating an upper-tropospheric ridge. A pattern of high probabilities for a negative T2m anomaly event appears a few days after the warm SST event (Fig. 3d), illustrating again a reversed relationship between the effect on European T2m based on cold and warm North Atlantic SST events.

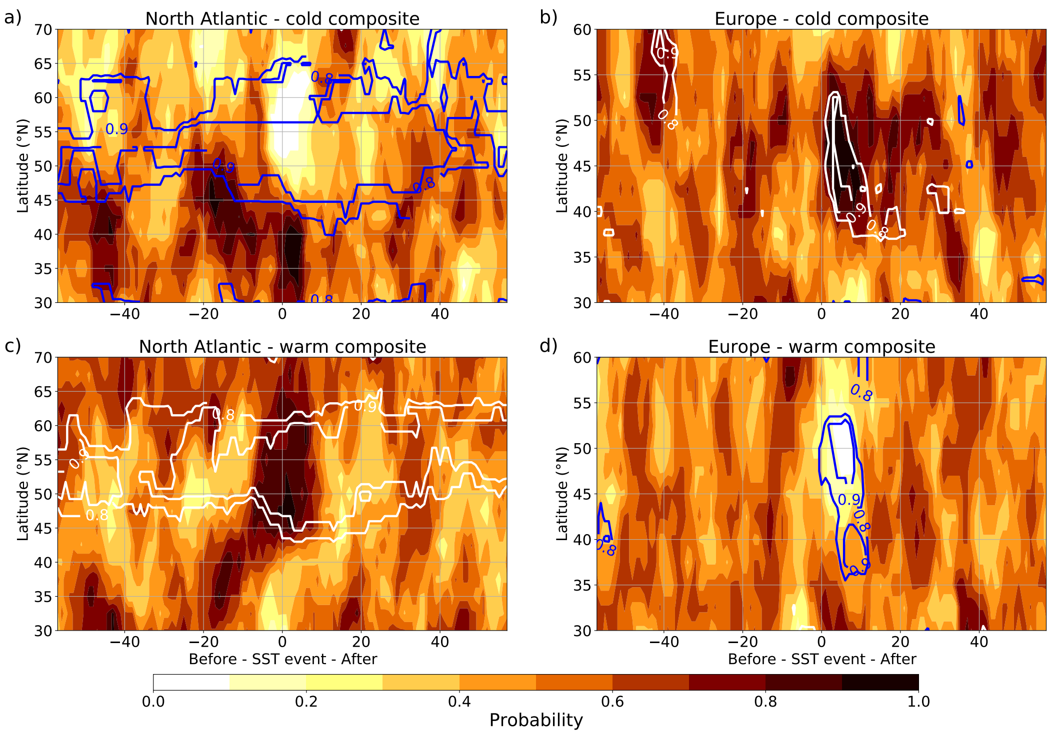

FIG. 3. Probabilities of positive Z300 anomalies (shading) and of positive/negative SST/T2m anomalies (contour - white/blue) above 0.8 of the a) North Atlantic average (15 - 40°W) for the composite mean of cold SST events and b) the European average (0 - 20°E) for the composite mean of cold SST events; c) and d) Same as a) and b) but for the composite mean of warm SST events.

Two to three weeks before the onset of the cold SST event we find patterns of a southward migration of the probability for positive Z300 anomalies which may contribute to the onset of the SST event (Fig. 3a). We identify a reversed pattern, i.e. a northward migration of the probability for positive Z300 anomalies before the onset of a warm SST event (Fig. 3c).

In the following we concentrate on the analysis of the composite of cold SST events, as the composite of warm SST events did not show any widespread and significant appearance of positive T2m anomalies over Europe. We average anomalies over the latitude band 40 - 60°N to study the propagation of high probability signals and estimate the duration of certain events within a longitudinal band (Fig. 4). Persistent patterns of probabilities with more than 90% for negative anomalies at lead/lag -60 and +60 in the North Atlantic emphasises again the presence of cold SSTs, which are likely to remain for a few weeks (Fig. 4a).

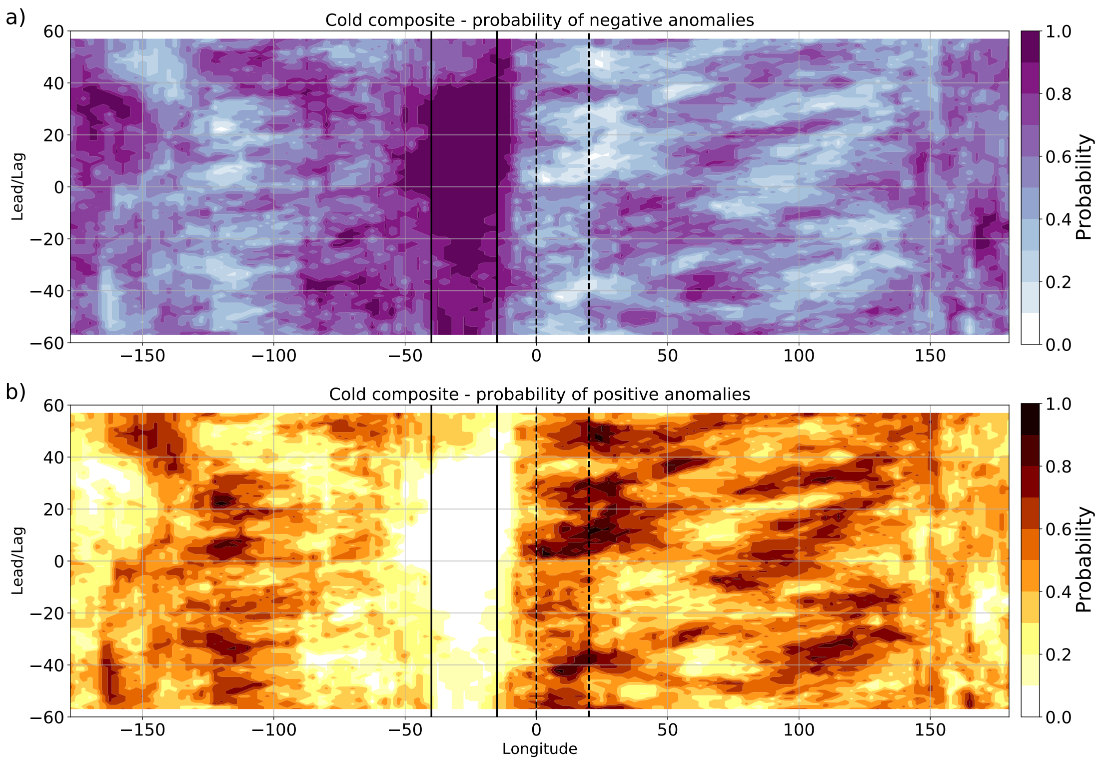

FIG. 4. Probabilities for negative anomalies (a)) and positive anomalies (b)) of SST (ocean) and T2m (continent) with respect to the composite mean of cold North Atlantic SST events after a latitudinal average over 40 - 60°N; solid vertical lines illustrate the longitude boundaries of the North Atlantic box and dashed lines the boundaries of the European box.

In the European longitudinal band (0 - 20°E) we find an area of near-zero probability for cold T2m anomalies immediately after the start date of the cold SST event. Instead, the mentioned area over central Europe is covered by high probabilities of up to 100% for positive T2m anomalies after the cold SST event (Fig. 4b). The probabilities indicate that the heat event is rapidly evolving over central Europe after the cold North Atlantic SST event and it persists for roughly one week. Subsequently, the temperature anomaly pattern starts to move towards Eastern Europe and decays east of the longitudinal range that we defined for central Europe.

We now turn to describing the evolution of heatwave conditions over Europe during the cold North Atlantic SST event using composites of different variables at lags near the cold SST event in order to capture the chronology as well as driving and contributing factors of the European heat events (Fig. 5 and 6).

In agreement with Fig. 4, we observe the formation of positive European T2m after lag 0, the start of the cold North Atlantic SST period (Fig. 5a). After ten days the anomaly pattern has already started moving towards Eastern Europe.

The upper tropospheric signal offers a similar time evolution: Until the cold SST event reaches its strongest values, the Eastern North Atlantic experiences an intensification of negative anomalies, likely associated with a strengthening of a trough (Fig. 5b). Around five days later, positive Z300 anomalies begin to form and spread over central Europe, leading to a trough-ridge pattern in the North Atlantic-European sector. This well developed dipole anomaly pattern favours the advection of warm subtropical air masses on the western flank of the European ridge. Ten days after the cold SST event we identify a reduced strength of the North Atlantic trough and an eastward shift of the ridge in correlation with the T2m anomaly pattern.

The fraction of total cloud cover reveals a reduction of up to 15% in the composite mean over central Europe after the cold SST event and an eastward movement subsequently in accordance to T2m and Z300 anomaly patterns (Fig. 5c).

Further, the anomaly of incoming net solar radiation is larger than net thermal radiation and the latent and sensible heat fluxes (Fig. 5d,e,f,g). Whereas the net incoming solar radiation reaches values locally of more than 25 Wm^{-2} over central Europe (Fig. 5f), the net thermal radiation is only able to oppose with approximately 5 Wm^{-2} over the same region (Fig. 5g). Therefore we obtain a net surface warming due to radiation.

Latent and sensible heat fluxes contribute with a magnitude similar to the thermal radiation over Europe (~5 Wm^{-2}), but they both point towards an upward heat flux leading to an additional warming of the near-surface atmospheric layer over the continent (Fig. 5d,e). A noticeable anomaly of the surface latent heat flux is found in the North Atlantic during the start date of the cold North Atlantic SST event (lag 0): increased negative anomalies of 15 to 20 Wm^{-2} result in an intensified upward heat flux and a cooling of the ocean (Fig. 5e).

In agreement with the negative latent heat flux anomalies, spatially and temporally coincident patterns of positive evaporation anomalies are present during and a few days after the onset of the cold SST anomaly (Fig. 6a).

A warming and increased moisture content in the near-surface layers of the atmosphere may drive an ascending air movement, potentially leading to an enhanced cloud cover. However, the total cloud cover does not exhibit any discernible signal here (Fig. 5c). Nevertheless, a vertical air movement can be mapped through a change in the cloud cover type. In fact, the North Atlantic box reveals a decline in the low cloud cover intensity of up to 8%, while the medium cloud cover fraction is increasing with values of up to 8% at lag 0 (Fig. 6c,d). In addition, we identify positive high cloud cover anomalies over Great Britain and towards the southwestern corner of the North Atlantic box at lag 0 with a similar magnitude (Fig. 6e).

The described positive anomaly patterns of medium and high cloud cover could explain ascending air movement and the band of positive large-scale precipitation anomalies, likely associated with a front, spanning from Great Britain through the North Atlantic basin until Newfoundland (Fig. 6b).

In conclusion of all parameters, the establishment of the North Atlantic trough in combination with evaporation, ascending air movement and precipitation along a frontal system over the North Atlantic occurs a few days prior to the generation of a European ridge and positive T2m anomalies of up to +3°C. Typically, we observe a reduced total cloud cover and increased incoming solar radiation over Europe. Surface latent and sensible heat fluxes over Europe contribute to an intensification of the European surface heat conditions, but the magnitude is not sufficient to explain a responsibility for the onset of European heat waves in the composite.

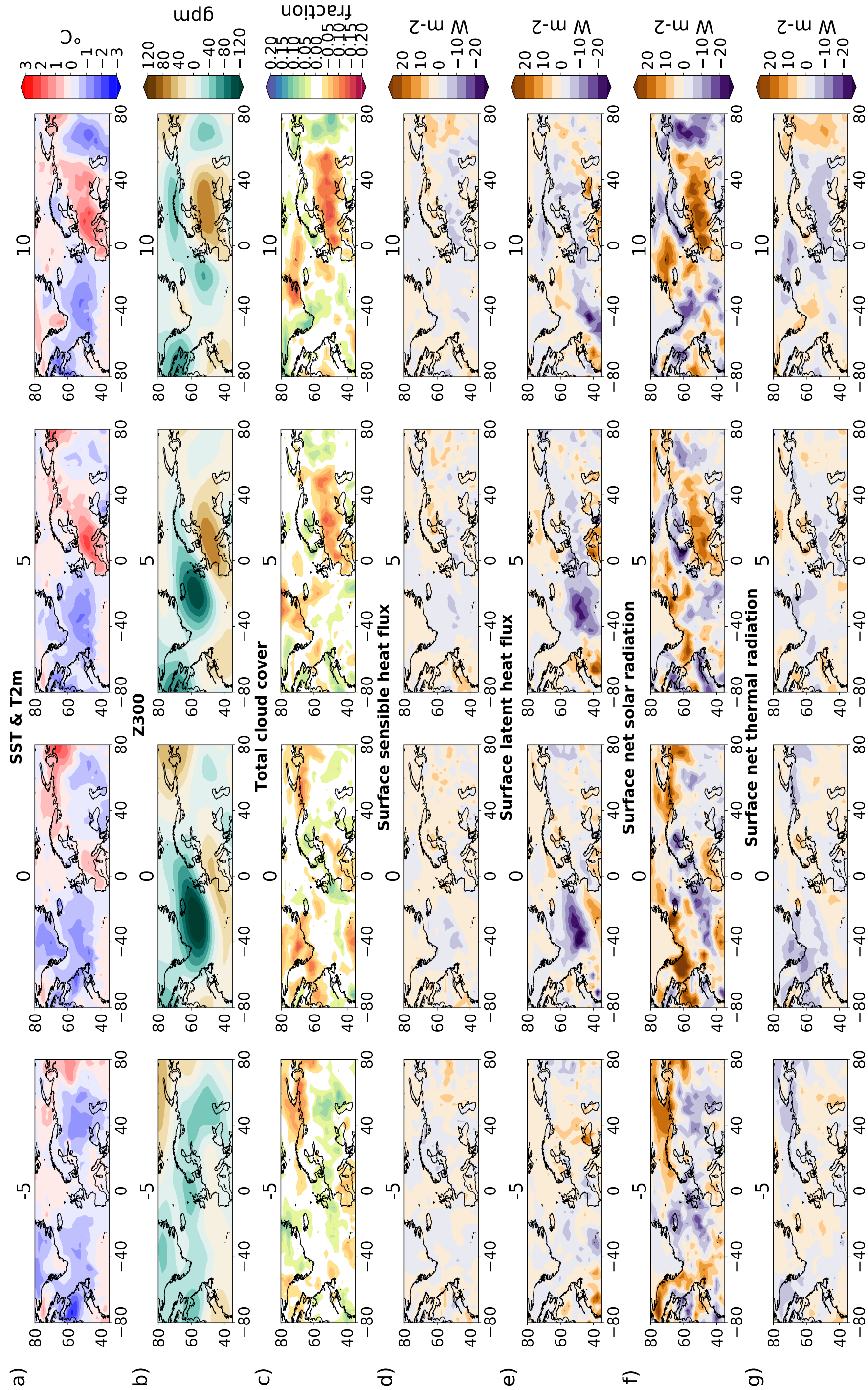

FIG. 5. Maps of composite mean of anomalies of different parameters 5 days before, during (0) and 5, 10 days after the North Atlantic cold SST events.

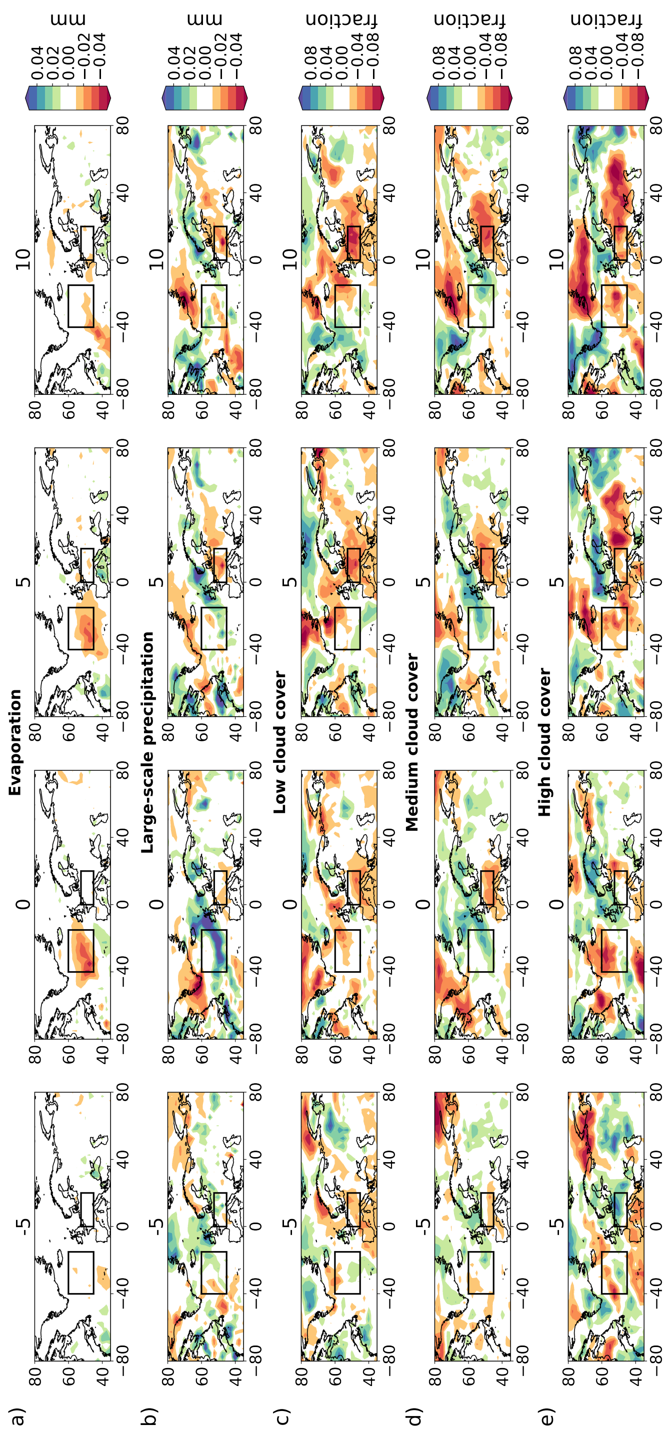

FIG. 6. Same as Fig.5, but with different parameters.

We now split the Z300 anomalies into the contribution of planetary waves (PW; wave number 1 to 3; Fig. 7c) and Rossby wave packets (RWP; wave number 4 to 15; Fig. 7d) to disentangle the contribution of different atmospheric waves.

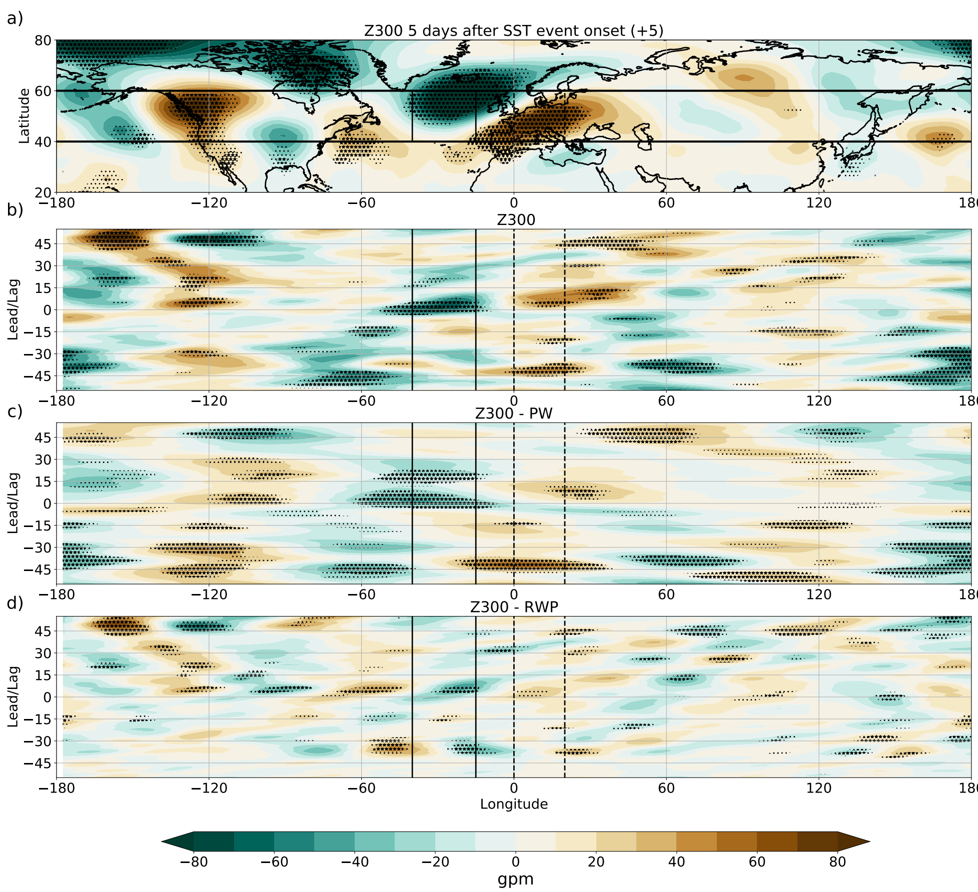

FIG. 7. a) Map of total Z300 5 days after the cold SST event onset; b) Hovmoller diagram of unfiltered Z300; c) Same as b) but for PW filtered Z300; d) Same as b) but for RWP filtered Z300; anomalies are based on a latitude average over 40 - 60°N (boundaries are shown as horizontal lines in a); solid vertical lines illustrate the longitude boundaries of the North Atlantic box and dashed lines the boundaries of the European box; Stars indicate significant values according to the Welch's T-test described in section 2d.

First, the unfiltered data displays a circumglobal wave pattern five days after the SST event onset with strongest anomalies of up to 80 gpm in the North Atlantic-European sector. Z300 anomalies of 60 to 70 gpm occur further upstream in the Arctic and the North American continent, whereas anomalies downstream over Asia reach only values of 20 gpm (Fig. 7a - enlargement of Fig. 5b over all longitudes).

The distinct trough-ridge pattern in the North Atlantic-European sector at around and after lag 0 is again outstanding in the Hovmoller diagram of the unfiltered Z300 data (Fig. 7b).

The filtered PW data unfolds maxima at 120°W, 0° and 120°E longitude with anomalies of up to +40 gpm, occurring mainly 45 to 25 days before the cold North Atlantic SST event (Fig. 7c). Together with significant negative anomalies in between these longitudes, this dominating pattern can be classified as a wave number 3 pattern. Up to 80% of the cases exhibit this pattern but with lower magnitude between -25 and 0 lag (see also Fig. A2 for the equivalent of Fig. 7c,d in terms of probability). Around lag 0 the pattern indicates an eastward shift, resulting in significantly negative Z300 anomalies prevailing in the North Atlantic longitude band. The pattern remains until 20 days after the cold SST event before it experiences a weakening and a westward shift.

The RWP anomalies generally show no significant signal pointing towards a hemisphere-wide wave pattern. Instead, regionally confined RWP activity becomes significant between 0° and 60°W five weeks before the cold SST event (Fig. 7d) , but the PW anomalies exhibit a reversed structure (Fig. 7c), canceling out a significant signal (Fig. 7b).

After the cold SST event onset, RWP activity occurs within the sector of North America and Europe, which superimposes the PW pattern in the North Atlantic-European sector, thus amplifying the signal. Approximately two weeks after the cold SST event the signal decreases and a westward movement evolves here as well.

Both PW and RWP activity seem to play important roles, as they show significant patterns around the cold SST event, adding up to a strong trough-ridge pattern. But it leaves the open question of the generation of the cold North Atlantic SST anomalies. Further it remains an open question whether the RWP energy is a result of a forward cascade of PW activity or whether surface and orographic forcing is relevant at this stage. Model-based studies with larger composite sizes are necessary for answering also the significant wave patterns 40 to 30 days prior to the cold SST event, as it might increase the predictability range.

b. *Upstream analysis of European T2m composite*

So far we have established the downstream analysis, studying the evolution of European T2m anomalies based on cold North Atlantic SST events. Now we continue by comparing the downstream and upstream analysis in order to check consistency between both approaches (Fig. 8). We study the individual paths of the composite and the overall JJA anomaly distribution of North Atlantic SSTs (blue bars) and European T2m (red bars).

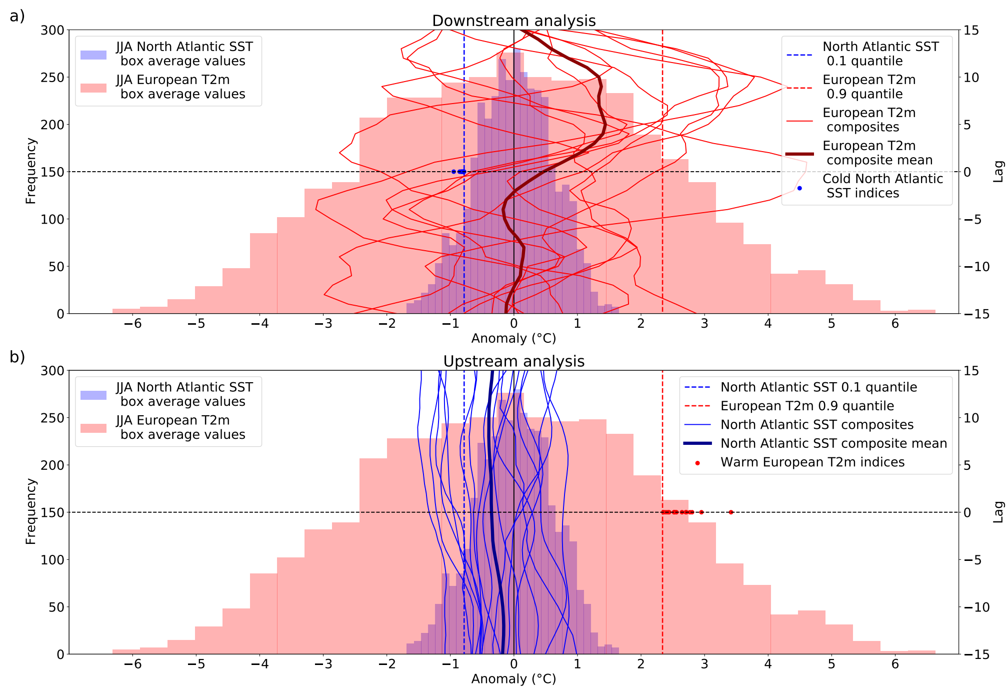

FIG. 8. Distribution of North Atlantic SST JJA box average (15 - 40°W, 45 - 60°N) (light blue) and of European T2m JJA box average (0 - 20°E, 45 - 52.5°N) (light red); both distributions are shown with an equal number of bins (30); the 0.1 quantile of the North Atlantic SST box average (dashed blue line) and the 0.9 quantile of the European T2m box average (dashed red line) are highlighted; cold North Atlantic SST events (blue dots) and corresponding European T2m composites (red lines) with the composite mean (thick dark red line) including the evolution related to the cold SST event are shown in the downstream analysis (a)); warm European T2m events (red dots) and corresponding North Atlantic SST (blue lines) with the composite mean (thick dark blue line) including the evolution related to the warm T2m event are shown in the upstream analysis (b)).

By using the daily JJA anomalies of the North Atlantic SST and the European T2m distribution, we find that both distributions are generally centred roughly around 0°C, but SST anomalies have much smaller variance than T2m anomalies.

Regarding the downstream analysis, we observe that the European T2m is distributed with almost half of the events on the positive and the other half on the negative anomaly side before the occurrence of a cold North Atlantic SST event (Fig. 8a). As the cold SST event approaches, the majority (ten of eleven) events shift towards positive T2m anomalies increasing the likelihood for the presence of a European heat wave after the start date of the cold North Atlantic SST event. Some of these events weaken after roughly a week and tend to return to an anomaly of 0°C, whereas other events reach their maximum a few days later.

Only a single event found in 1985 turned towards negative T2m anomalies after the cold SST event. Five days after the cold SST event, we identify a trough which spreads from the North Atlantic into Europe during this event in August 1985 (Fig. A3b). A ridge and above average temperatures were present downstream of this trough too, but here located over northwestern parts of Russia in this particular year.

In general, the distribution shifts towards positive T2m anomalies a few days after a cold SST event and in Table 1 we identified that five of eleven events identified in the downstream analysis are in fact associated with a heat wave.

We now turn to studying the evolution of North Atlantic SST anomalies before and after positive European T2m anomalies. We observe that the composite mean of the 17 European heat events identified in this study is associated with negative North Atlantic SST anomalies (Fig. 8b). The majority (eleven of 17) of heat events are accompanied by below-average North Atlantic SSTs: five out of 17 heat waves in fact occurred with a preceding strong cold North Atlantic SST anomaly. Another 6 heat waves are accompanied by weaker cold SST anomalies and the remaining six heat waves are associated with positive SST anomalies.

The low frequent variability of the North Atlantic SST provides a challenge to argue that a cold North Atlantic SST event really happens prior to the occurrence of the European heat events in the upstream analysis.

The downstream analysis confirm that the European T2m experiences a shift towards positive anomalies which increases the probability for heat waves, whilst the upstream method namely shows a slight preference for cold North Atlantic SSTs (eleven of 17), but not for the vast majority. Hence, we emphasise that North Atlantic SSTs are one factor among different European heat wave drivers, but if once an anomalously cold North Atlantic SST anomaly evolved during summer, it is very likely to be associated with positive European T2m anomalies and with an increased probability for a heat wave.

For the sake of completeness, we performed the same analysis for warm North Atlantic SST events and cold European T2m events (Fig. A4). We found a shift of the temperature distribution towards negative European T2m values in the downstream analysis (Fig. A4a) and a shift towards positive SST values in the upstream analysis (Fig. A4b), suggesting an opposite signature of the European temperature distribution shift with regard to the North Atlantic SST state. Further we conclude a reduced probability of European heat waves during and after warm North Atlantic SST events.

5. Discussion

The performed two-sided analysis in the Euro-Atlantic sector reveals that cold North Atlantic SSTs are associated with a shift in the European surface temperature distribution towards warmer temperatures and a higher likelihood for heat waves. Specifically, the downstream analysis (Fig. 8a), but also in combination with the upstream method (Fig. 8b), suggest temperature maxima over Europe a few days after a cold SST event onset.

The above mentioned temporally uneven distribution between cold and warm SST events (Fig. 1c) likely arises due to an imprint of the Atlantic multi-decadal variability (AMV). It is remarkable that only two of the eleven cold SST events are found in the 20-year long period during 1995 and 2014, which is part of the positive AMV phase and makes up almost half of the data set. Based on our results that North Atlantic SSTs modify the temporal distribution of European heat waves, a negative AMV phase could remotely contribute to a European summer temperature distribution shift towards a higher probability of heat wave occurrences.

Although it's challenging to relate a daily minimum of a low frequently varying parameter (North Atlantic SST) to a daily maximum of a parameter of higher frequency (European T2m) (Fig. 4), we are able to identify a statistical relationship between these parameters during boreal summer (Fig. 2a,b, 8a). But confirming a significant increase of the European heat wave frequency during the cold phase of the AMV requires a higher number of European heat waves tested as well as more AMV cycles analysed.

Despite our small sample size, the results we find in our study are significant around the time of the SST events. However, a higher sample size would provide a reliable quantitative statement about the strength of the shift in the European temperature distribution. An evaluation about this would provide information about whether the shift is in relationship with changes in the Atlantic ocean circulation. Further this distribution shift can be compared with the evident upward trend in the temperature distribution due to global warming (Donat and Alexander 2012; Thornton et al. 2014).

The study by Cassou et al. (2005) poses that a global shift in the temperature distribution is in line with an increase in the occurrence of extreme warm days mainly associated with the European Blocking or the Atlantic Low regime. The former pattern is characterised by an anomalously strong ridge over northern Europe without the presence of a well-developed trough over the North Atlantic.

The trough-ridge pattern in the North Atlantic-European sector we find some days after the cold North Atlantic SST event (Fig. 2, 3, 5b, 7a,b) much better resembles the Atlantic-Low regime, which was present during previous heat waves like in 1994. Cassou et al. (2005) showed that early summer hot conditions over western and central Europe associated with the Atlantic Low pattern could be mapped out through the presence of a Rossby wave train. Our wave analysis supports this mechanism, as the RWP activity after the cold North Atlantic SST onset is in alignment with the trough-ridge pattern in the North Atlantic-European sector (Fig. 8b,d).

A previous case study about the European heat wave in 2018 concludes that not only the Atlantic Low pattern, but also the persistent blocking regime both were main contributors, however, an interdependence and a positive correlation complicate a separately performed evaluation (Kueh and Lin 2020).

Beside the cold North Atlantic SST anomaly within the box studied, a warm SST anomaly to the south as found in summer 2018 (Fig. 1a) contributes to an increased meridional SST gradient in the North Atlantic. This could result in enhanced atmospheric baroclinicity, which is followed by an unusually strong southward shift of the North Atlantic jet stream as proposed by Duchez et al. (2016). Another study exemplified that the southward jet stream shift in the North Atlantic is connected with a northward displacement of the jet stream in western Europe, potentially fostering the establishment of high pressure and temperature extremes downstream over central Europe (Josey et al. 2018). Particularly the Z300 anomaly patterns (Fig. 5b) demonstrate a non-simultaneous strengthening of the North Atlantic trough and the European ridge. The observed delayed European ridge development seems to constitute the downstream response of the southward jet stream shift in the North Atlantic.

Surface heat fluxes and soil moisture do not play a major role over the European continent in our downstream composite study (Fig. 5). Long term changes in the soil moisture content are not proposed to be a major factor in forcing the atmospheric circulation and associated high-pressure systems over Europe (Findell and Delworth 2005). Nonetheless a forcing due to local thermodynamical surface effects is not negligible, as it could play a more important role in amplifying European heat waves and it's relevant for the heat loss over the North Atlantic ocean as well.

The composite of cold North Atlantic SST events in the downstream analysis suggests that the oceanic heat loss over the North Atlantic is associated with evaporation, an ascending air movement and precipitation, likely occurring in frontal systems (Fig. 5 and 6). The study by Zschenderlein et al. (2020) used a Lagrangian analysis with backward trajectories and identified that a similar sequence of processes is happening in their so called "remote heating branch" with its origin in the North Atlantic as well. The described branch further involves diabatic heating through the release of latent heat by stratiform precipitation, which facilitates the onset of an upper-tropospheric anticyclone over Europe and is thus connected to European heat waves. This is another process that could describe the delayed European ridge amplification relative to the setup of the North Atlantic trough and the associated precipitation band along the observed frontal system (Fig. 2, 3, 5b, 6b, 7a,b).

Further analysis and model experiments are necessary to separate the relative contributions of thermodynamical drivers like surface fluxes and diabatic heating and dynamical drivers like atmospheric waves, and to understand specifically the mechanism between North Atlantic SSTs and the atmospheric circulation, potentially leading to European heat waves.

6. Conclusion and Outlook

Apart from previous case-study based analysis, our study provides a first estimate on how the North Atlantic SST state could generally modify the European surface temperature distribution during boreal summer. By performing a two-sided composite study, consisting of an up- and downstream analysis in the North Atlantic European sector, we find the results as followed:

1.) The downstream analysis reveals that cold North Atlantic SSTs are connected with a shift in the European summer temperature distribution towards positive anomalies a few days after the cold SST event. Five out of 11 cold North Atlantic SST events are followed by a European heat wave a few days later. A North Atlantic trough accompanied by a European ridge build up consecutively.

2.) The upstream analysis discloses that eleven of 17 European heat waves are co-existent with cold North Atlantic SSTs. A comparison between up- and downstream analysis shows that five of 17 European heat waves within the period of 1979 to 2019 could be related to cold North Atlantic SST below the 0.1 quantile a few days in advance.

3.) The warm North Atlantic SST events are related to European trough conditions and negative T2m anomalies a few days later, suggesting an approximately linear relationship between the central European T2m and the North Atlantic SST state.

4.) Reduced total cloud cover and enhanced incoming net solar radiation subsequent to the cold North Atlantic SST event support central European heat wave conditions. Latent and sensible heat fluxes do not play a triggering role over the European continent, but may amplify the European conditions. Moreover, latent heat release associated with evaporation could initiate ascending air movement and precipitation over the North Atlantic, connected to diabatic heating injected into the upper troposphere over Europe, fostering European heat waves.

5.) For disentangling the contribution of different wave structures and its spatial extent we perform an atmospheric wave filtering into planetary waves (wave number one to three) and

Rossby wave packets (wave numbers four to 15). It unravels a predominant wavenumber three pattern and a regionally confined Rossby wave packet superimposed, leading to the trough-ridge pattern in the North Atlantic-European sector. The results highlight the importance of analysing both wave types simultaneously.

6.) The detected atmospheric trough-ridge pattern closely resembles the Atlantic Low regime, which is found to be responsible for a number of European heat wave occurrences in previous studies.

The results of our study highlight the role of the North Atlantic SST in modifying the European T2m and contribute to an improved understanding of a lagged statistical relationship between atmosphere and ocean interaction. However, additional analysis and model-based studies are required to fully understand the causal mechanism. Further investigation of the low frequently varying North Atlantic SST is essential, as very low North Atlantic SSTs could be dynamically or thermodynamically linked to the Atlantic Low regime development. Moreover the North Atlantic SSTs potentially provide greater predictability of European heat waves.

Acknowledgments. We thank the European Centre for Medium-Range Weather Forecasts (ECMWF) data server for the freely available ERA5 reanalysis data.

Data availability statement. ERA5 reanalysis data on single levels from 1979 to 2019 used in this study was freely retrieved from: `https://cds.climate.copernicus.eu/cdsapp#!/dataset/reanalysis-era5-single-levels?tab=form`.

Notebooks about the data analysis are freely accessible through: `https://github.com/jukrueger/ERA5-NASST-EuroHW`.

APPENDIX

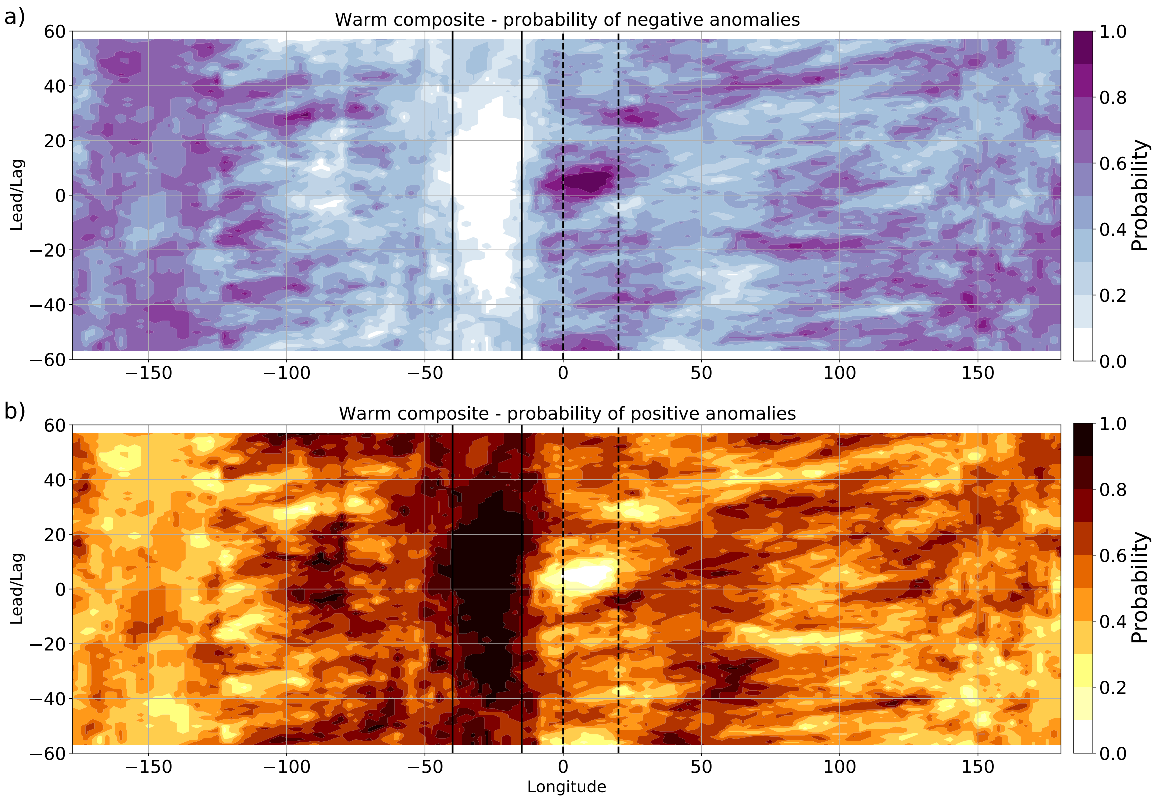

FIG. A1. Same as Fig. 4, but here for composite mean of warm North Atlantic SSTs.

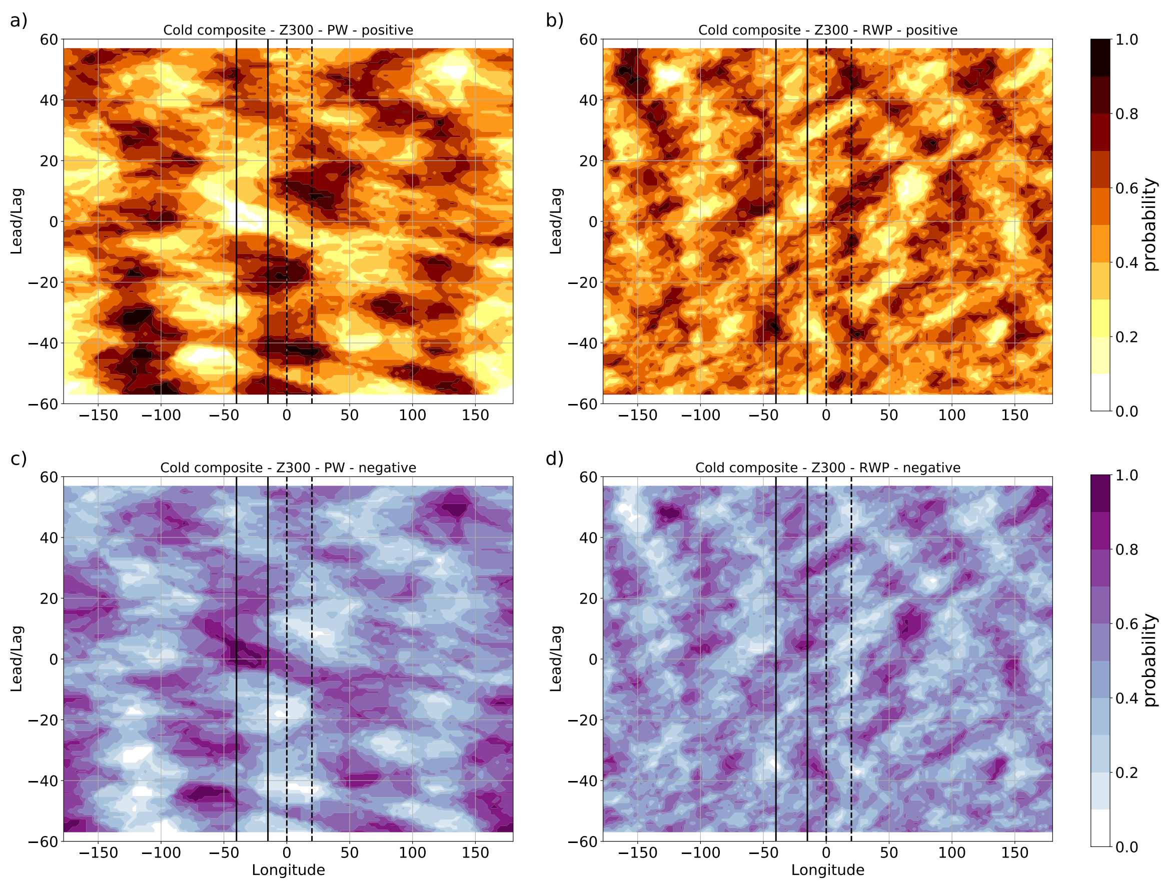

FIG. A2. Probabilities for positive (a) and b)) and negative (c) and d)) anomalies of filtered PW (a) and c)) and RWP (b) and d)) based on Z300 for the composite of cold North Atlantic SSTs; solid vertical lines illustrate the longitude boundaries of the North Atlantic box and dashed lines the boundaries of the European box.

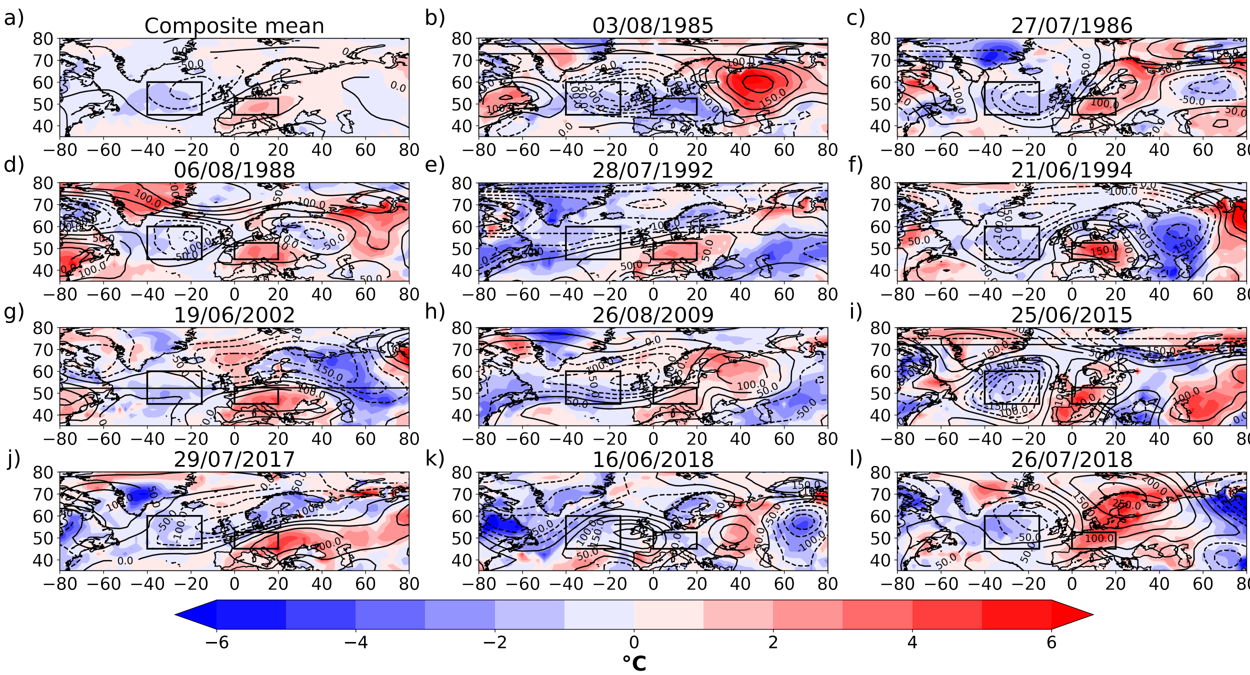

FIG. A3. Maps of SST (ocean) and T2m (continent; coloured) and Z300 (contours) anomalies based on the state of five days after the respective cold North Atlantic SST event; a) depicts the composite mean and the remaining figures display the state of each of the eleven composite cases; the title includes the respective date of the cold North Atlantic SST event consistent with the dates listed in Table 1.

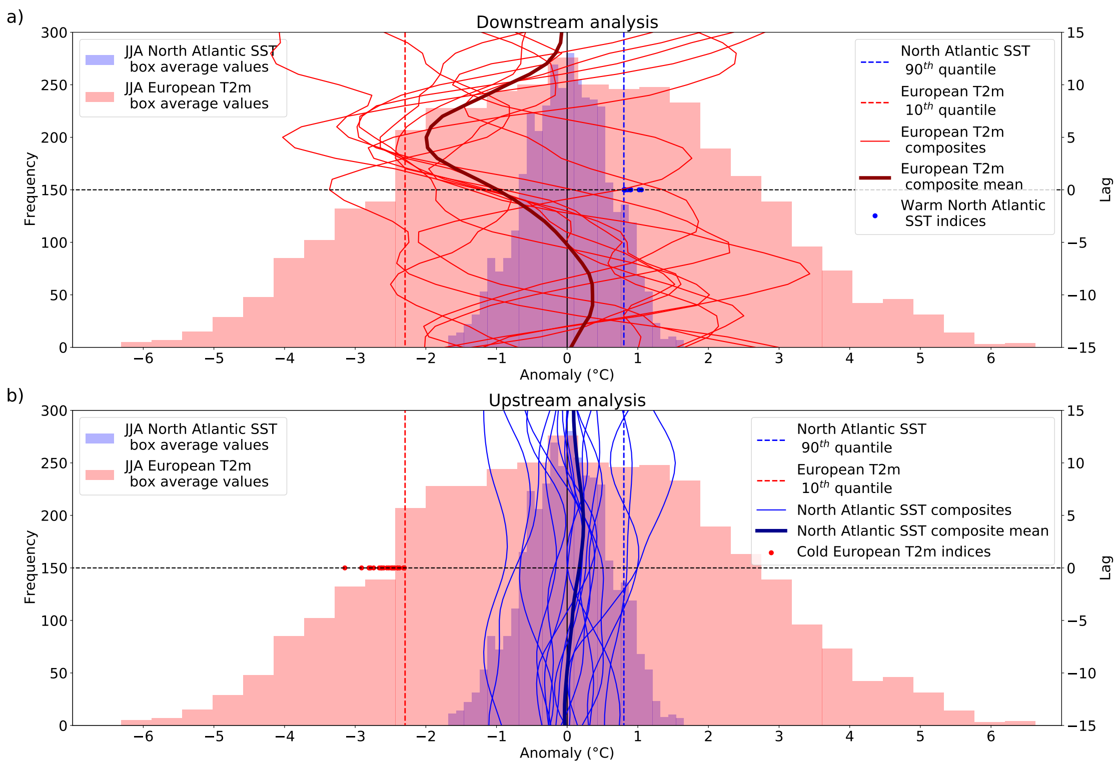

FIG. A4. Same as in Fig. 8; but here the 0.9 quantile of the North Atlantic SST box average (dashed blue line) and the 0.1 quantile of the European T2m JJA box average (dashed red line) are shown as we show up the European T2m composites (red lines) with its composite mean (thick dark red line) based on warm North Atlantic SST events (blue dots) in the downstream analysis (a)) and we show up the North Atlantic SST composites (blue lines) with its composite mean (thick dark blue line) based on cold European T2m events (red dots) in the upstream analysis (b)).

References

Barriopedro, D., E. Fischer, J. Luterbacher, R. Trigo, and R. García-Herrera, 2011: The Hot Summer of 2010: Redrawing the Temperature Record Map of Europe. *Science (New York, N.Y.)*, **332**, 220–4, https://doi.org/10.1126/science.1201224.

Black, E., M. Blackburn, G. Harrison, B. Hoskins, and J. Methven, 2004: Factors contributing to the summer 2003 European heatwave. *Weather*, **59 (8)**, 217–223, https://doi.org/10.1256/wea.74.04.

Brönnimann, S., 2007: Impact of El Niño-Southern Oscillation on European climate. *Rev. Geophys.*, **45 (3)**, https://doi.org/10.1029/2006RG000199.

Cassou, C., L. Terray, and A. S. Phillips, 2005: Tropical Atlantic Influence on European Heat Waves. *J. Climate*, **18 (15)**, 2805–2811, https://doi.org/10.1175/jcli3506.1.

Chang, E. K., 1993: Downstream development of baroclinic waves as inferred from regression analysis. *Journal of the Atmospheric Sciences*, **50 (13)**, 2038–2053, https://doi.org/10.1175/1520-0469(1993)050<2038:DDOBWA>2.0.CO;2.

Christidis, N., G. S. Jones, and P. A. Stott, 2015: Dramatically increasing chance of extremely hot summers since the 2003 European heatwave. *Nature Climate Change*, **5 (1)**, 46–50, https://doi.org/https://doi.org/10.1038/nclimate2468.

Coumou, D., and S. Rahmstorf, 2012: A decade of weather extremes. *Nature Climate Change*, **2 (7)**, 491–496, https://doi.org/https://doi.org/10.1038/nclimate1452.

Coumou, D., A. Robinson, and S. Rahmstorf, 2013: Global increase in record-breaking monthly-mean temperatures. *Climatic Change*, **118 (3)**, 771–782, https://doi.org/10.1007/s10584-012-0668-1.

Diffenbaugh, N. S., and Coauthors, 2017: Quantifying the influence of global warming on unprecedented extreme climate events. *Proc Natl Acad Sci USA*, **114 (19)**, 4881, https://doi.org/10.1073/pnas.1618082114.

Donat, M. G., and L. V. Alexander, 2012: The shifting probability distribution of global daytime and night-time temperatures. *Geophys. Res. Lett.*, **39 (14)**, L14 707, https://doi.org/10.1029/2012GL052459.

Dong, B., R. Sutton, L. Shaffrey, and L. Wilcox, 2016: The 2015 European Heat Wave. *Bull. Amer. Meteor. Soc.*, **97 (12)**, S57–S62, https://doi.org/10.1175/bams-d-16-0140.1.

Duchez, A., and Coauthors, 2016: Drivers of exceptionally cold North Atlantic Ocean temperatures and their link to the 2015 European heat wave. *Environmental Research Letters*, **11**, 074 004, https://doi.org/10.1088/1748-9326/11/7/074004.

Dunstone, N., D. Smith, S. Hardiman, R. Eade, M. Gordon, L. Hermanson, G. Kay, and A. Scaife, 2019: Skilful Real-Time Seasonal Forecasts of the Dry Northern European Summer 2018. *Geophys. Res. Lett.*, **46 (21)**, 12 368–12 376, https://doi.org/10.1029/2019gl084659.

Findell, K. L., and T. L. Delworth, 2005: A modeling study of dynamic and thermodynamic mechanisms for summer drying in response to global warming. *Geophys. Res. Lett.*, **32 (16)**, L16 702, https://doi.org/10.1029/2005GL023414.

Fischer, E. M., S. I. Seneviratne, P. L. Vidale, D. Lüthi, and C. Schär, 2007: Soil Moisture-Atmosphere Interactions during the European Summer Heat Wave. *J. Climate*, **20 (20)**, 5081–5099, https://doi.org/10.1175/jcli4288.1.

Fragkoulidis, G., V. Wirth, P. Bossmann, and A. H. Fink, 2018: Linking Northern Hemisphere temperature extremes to Rossby wave packets. *Q.J.R. Meteorol. Soc.*, **144 (711)**, 553–566, https://doi.org/10.1002/qj.3228.

García-Herrera, R., J. Díaz, R. Trigo, J. Luterbacher, and E. Fischer, 2010: A Review of the European Summer Heat Wave of 2003. *Critical Reviews in Environmental Science and Technology*, **40**, 267–306, https://doi.org/10.1080/10643380802238137.

Grumm, R. H., 2011: The Central European and Russian Heat Event of July-August 2010. *Bull. Amer. Meteor. Soc.*, **92 (10)**, 1285–1296, https://doi.org/10.1175/2011bams3174.1.

Hauser, M., R. Orth, and S. I. Seneviratne, 2016: Role of soil moisture versus recent climate change for the 2010 heat wave in western Russia. *Geophys. Res. Lett.*, **43 (6)**, 2819–2826, https://doi.org/10.1002/2016GL068036.

Hersbach, H., and Coauthors, 2020: The ERA5 global reanalysis. *Q.J.R. Meteorol. Soc.*, **146 (730)**, 1999–2049, https://doi.org/10.1002/qj.3803.

Josey, S. A., J. J.-M. Hirschi, B. Sinha, A. Duchez, J. P. Grist, and R. Marsh, 2018: The Recent Atlantic Cold Anomaly: Causes, Consequences, and Related Phenomena. *Annu. Rev. Mar. Sci.*, **10 (1)**, 475–501, https://doi.org/10.1146/annurev-marine-121916-063102.

Kueh, M.-T., and C.-Y. Lin, 2020: The 2018 summer heatwaves over northwestern Europe and its extended-range prediction. *Scientific Reports*, **10 (1)**, 19 283, https://doi.org/10.1038/s41598-020-76181-4.

Lee, S., and I. M. Held, 1993: Baroclinic wave packets in models and observations. *Journal of the Atmospheric Sciences*, **50 (10)**, 1413–1428, https://doi.org/10.1175/1520-0469(1993)050<1413:BWPIMA>2.0.CO;2.

Lhotka, O., and J. Kyselý, 2015: Characterizing joint effects of spatial extent, temperature magnitude and duration of heat waves and cold spells over Central Europe. *Int. J. Climatol.*, **35 (7)**, 1232–1244, https://doi.org/10.1002/joc.4050.

Liu, Q., 1994: On the definition and persistence of blocking. *Tellus A*, **46 (3)**, 286–298, https://doi.org/10.1034/j.1600-0870.1994.t01-2-00004.x.

Mann, M. E., S. Rahmstorf, K. Kornhuber, B. A. Steinman, S. K. Miller, S. Petri, and D. Coumou, 2018: Projected changes in persistent extreme summer weather events: The role of quasi-resonant amplification. *Science advances*, **4 (10)**, eaat3272–eaat3272, https://doi.org/10.1126/sciadv.aat3272.

McCarthy, M., and Coauthors, 2019: Drivers of the UK summer heatwave of 2018. *Weather*, **74 (11)**, 390–396, https://doi.org/10.1002/wea.3628.

Mecking, J. V., S. S. Drijfhout, J. J.-M. Hirschi, and A. T. Blaker, 2019: Ocean and atmosphere influence on the 2015 European heatwave. *Environmental Research Letters*, **14 (11)**, 114 035, https://doi.org/10.1088/1748-9326/ab4d33.

Miller, S., K. Chua, J. Coggins, and H. Mohtadi, 2021: Heat Waves, Climate Change, and Economic Output. *Journal of the European Economic Association*, **19 (5)**, 2658–2694, https://doi.org/10.1093/jeea/jvab009.

Pilch Kedzierski, R., K. Matthes, and K. Bumke, 2020: New insights into Rossby wave packet properties in the extratropical UTLS using GNSS radio occultations. *ACP*, **20 (19)**, 11 569–11 592, https://doi.org/10.5194/acp-20-11569-2020.

Robine, J.-M., K. Cheung, S. Roy, H. Oyen, C. Griffiths, j.-p. Michel, and F. Herrmann, 2008: Death toll exceeded 70,000 in Europe during the summer of 2003. *Comptes rendus biologies*, **331**, 171–8, https://doi.org/10.1016/j.crvi.2007.12.001.

Röthlisberger, M., L. Frossard, L. F. Bosart, D. Keyser, and O. Martius, 2019: Recurrent Synoptic-Scale Rossby Wave Patterns and Their Effect on the Persistence of Cold and Hot Spells. *J. Climate*, **32 (11)**, 3207–3226, https://doi.org/10.1175/JCLI-D-18-0664.1.

Röthlisberger, M., S. Pfahl, and O. Martius, 2016: Regional-scale jet waviness modulates the occurrence of midlatitude weather extremes. *Geophys. Res. Lett.*, **43 (20)**, 10,989–10,997, https://doi.org/10.1002/2016GL070944.

Schär, C., P. L. Vidale, D. Lüthi, C. Frei, C. Häberli, M. Liniger, and C. Appenzeller, 2004: 2004: The role of increasing temperature variability in European summer heatwaves. *Nature*, **427**, 332–6, https://doi.org/10.1038/nature02300.

Sinclair, V. A., J. Mikkola, M. Rantanen, and J. Räisänen, 2019: The summer 2018 heatwave in Finland. *Weather*, **74 (11)**, 403–409, https://doi.org/10.1002/wea.3525.

Steinfeld, D., M. Boettcher, R. Forbes, and S. Pfahl, 2020: The sensitivity of atmospheric blocking to upstream latent heating - numerical experiments. *WCD*, **1 (2)**, 405–426, https://doi.org/10.5194/wcd-1-405-2020.

Steinfeld, D., and S. Pfahl, 2019: The role of latent heating in atmospheric blocking dynamics: a global climatology. *Climate Dynamics*, **53**, pages 6159–6180, https://doi.org/10.1007/s00382-019-04919-6.

Stott, P. A., D. A. Stone, and M. R. Allen, 2004: Human contribution to the European heatwave of 2003. *Nature*, **432 (7017)**, 610–614, https://doi.org/10.1038/nature03089.

Stott, P. A., and Coauthors, 2016: Attribution of extreme weather and climate-related events. *WIREs Clim Change*, **7 (1)**, 23–41, https://doi.org/10.1002/wcc.380.

Suarez-Gutierrez, L., W. A. Müller, C. Li, and J. Marotzke, 2020: Dynamical and thermodynamical drivers of variability in European summer heat extremes. *Climate Dynamics*, **54 (9)**, 4351–4366, https://doi.org/10.1007/s00382-020-05233-2.

Sun, Q., C. Miao, M. Hanel, A. G. L. Borthwick, Q. Duan, D. Ji, and H. Li, 2019: Global heat stress on health, wildfires, and agricultural crops under different levels of climate warming. *Environment International*, **128**, 125–136, https://doi.org/10.1016/j.envint.2019.04.025.

Sutton, R. T., and D. L. R. Hodson, 2005: Atlantic Ocean Forcing of North American and European Summer Climate. *Science*, **309 (5731)**, 115, https://doi.org/10.1126/science.1109496.

Thornton, P., P. Ericksen, M. Herrero, and A. Challinor, 2014: Climate Variability and Vulnerability to Climate Change: A Review. *Global change biology*, **20 (11)**, 3313–3328, https://doi.org/10.1111/gcb.12581.

Wirth, V., M. Riemer, E. K. M. Chang, and O. Martius, 2018: Rossby Wave Packets on the Midlatitude Waveguide–A Review. *Mon. Wea. Rev.*, **146 (7)**, 1965–2001, https://doi.org/10.1175/MWR-D-16-0483.1.

Wolf, G., and V. Wirth, 2017: Diagnosing the Horizontal Propagation of Rossby Wave Packets along the Midlatitude Waveguide. *Monthly Weather Review*, **145**, 3247–3264, https://doi.org/10.1175/MWR-D-16-0355.1.

Zimin, A., I. Szunyogh, D. Patil, B. Hunt, and E. Ott, 2003: Extracting Envelopes of Rossby Wave Packets. *Monthly Weather Review*, **131**, 1011–1017, https://doi.org/10.1175/MWR3122.1.

Zschenderlein, P., A. H. Fink, S. Pfahl, and H. Wernli, 2019: Processes determining heat waves across different European climates. *Q.J.R. Meteorol. Soc.*, **145 (724)**, 2973–2989, https://doi.org/10.1002/qj.3599.

Zschenderlein, P., S. Pfahl, H. Wernli, and A. H. Fink, 2020: A Lagrangian analysis of upper-tropospheric anticyclones associated with heat waves in Europe. *WCD*, **1 (1)**, 191–206, https://doi.org/10.5194/wcd-1-191-2020.